Class I and class III phosphoinositide 3-kinases are required for actin polymerization that propels phagosomes

Michal Bohdanowicz,[1] Gabriela Cosío,[1] Jonathan M. Backer,[2] and Sergio Grinstein[1]

[1]Division of Cell Biology, Hospital for Sick Children, Toronto, Ontario M5G 1X8, Canada
[2]Department of Molecular Pharmacology, Albert Einstein College of Medicine, Bronx, NY 10461

Actin polymerization drives the extension of pseudopods that trap and engulf phagocytic targets. The polymerized actin subsequently dissociates as the phagocytic vacuole seals and detaches from the plasma membrane. We found that phagosomes formed by engagement of integrins that serve as complement receptors (CR3) undergo secondary waves of actin polymerization, leading to the formation of "comet tails" that propel the vacuoles inside the cells. Actin tail formation was accompanied by and required de novo formation of $PI(3,4)P_2$ and $PI(3,4,5)P_3$ on the phagosomal membrane by class I phosphoinositide 3-kinases (PI3Ks). Although the phosphatidylinositide phosphatase Inpp5B was recruited to nascent phagosomes, it rapidly detached from the membrane after phagosomes sealed. Detachment of Inpp5B required the formation of PI(3)P. Thus, class III PI3K activity was also required for the accumulation of $PI(4,5)P_2$ and $PI(3,4,5)P_3$ and for actin tail formation. These experiments reveal a new PI(3)P-sensitive pathway leading to $PI(3,4)P_2$ and $PI(3,4,5)P_3$ formation and signaling in endomembranes.

Introduction

Removal of foreign particles by phagocytosis plays a central role in innate immunity (Aderem and Underhill, 1999). Phagocytosis also mediates the clearance of apoptotic bodies that is essential for tissue remodeling and homeostasis (Zhou and Yu, 2008). Mammalian cells express two types of phagocytic receptors: nonopsonic receptors that bind directly to the particle and receptors that recognize opsonins, serum components such as antibodies or complement which coat the target. The most widely studied opsonic receptors are Fcγ receptors (FcγRs), which bind the Fc portion of IgG, and CR3, which bind the C3bi component of complement (Underhill and Ozinsky, 2002).

FcγRs and CR3 differ not only in the nature of their ligands but also in their mode of signaling. Although FcγRs engage Src-family and Syk kinases, these steps are not essential for CR3-mediated phagocytosis (Aderem and Underhill, 1999). Nevertheless, the signal transduction pathways of both receptors ultimately converge, eliciting actin remodeling that leads to particle engulfment. Rho-family GTPases mediate actin polymerization in both instances, although the identity of the specific GTPases involved remains the subject of controversy (Caron and Hall, 1998; Hall et al., 2006). A strict requirement for phosphatidylinositol-(3,4,5)-trisphosphate ($PI(3,4,5)P_3$) is another common feature of the phagocytosis of large particles by FcγR and CR3.

The actin accumulated around nascent phagosomes depolymerizes within minutes of internalization, a step that is believed to be required for unimpeded fusion of endomembranes with the maturing vacuole (Liebl and Griffiths, 2009). In the case of FcγR-induced internalization, F-actin is only detectable at later stages, very transiently, around <8% of phagosomes (Liebl and Griffiths, 2009). However, in the course of analyzing the fate of phagosomes formed via CR3, we noted the regular occurrence of a second wave of actin polymerization around fully internalized phagosomes. We describe the mechanism underlying this event, which involves the conversion of

M. Bohdanowicz and G. Cosío contributed equally to this paper.

Correspondence to Sergio Grinstein: sergio.grinstein@sickkids.ca

Abbreviations used in this paper: DN, dominant negative; FcγR, Fcγ receptor; FKBP, FK506-binding protein; LDR, Lyn11-directed rapamycin-binding domain; PBD, p21-binding domain; PH, pleckstrin homology; YF, YFP-FKBP.

The Rockefeller University Press $30.00
J. Cell Biol. Vol. 191 No. 5 999–1012
www.jcb.org/cgi/doi/10.1083/jcb.201004005

phosphatidylinositol-(4,5)-bisphosphate ($PI(4,5)P_2$) to $PI(3,4,5)P_3$ by class I phosphoinositide 3-kinases (PI3Ks), the dislodgement of the 5′-phosphoinositide phosphatase, Inpp5B, by phosphatidylinositol-(3)-phosphate (PI(3)P) to allow accumulation of both $PI(4,5)P_2$ and $PI(3,4,5)P_3$, and the reengagement of Rho-family GTPases to form actin tails that propel phagosomes inside the macrophage.

Results

Actin-tailed phagosomes form after CR3-mediated phagocytosis

The actin-driven process that results in the engulfment of C3bi-coated particles is unclear; earlier studies suggested that particles sink into the cytosol of the phagocyte (Kaplan, 1977; Aderem and Underhill, 1999), whereas more recent observations postulated entrapment by thin pseudopods that wrap around the particles (Hall et al., 2006). We reanalyzed this question by continuously monitoring actin distribution in RAW264.7 macrophages stably transfected with either mCherry- or GFP-actin that were challenged by C3bi-coated RBCs. Our observations replicated the extension of thin, actin-rich structures that surrounded and entrapped the target particles (Video 1). Such actin accumulation at the plasma membrane dissipated shortly after completion of phagocytosis. More remarkably however, we noted the development of secondary waves of actin polymerization in association with most formed phagosomes (Fig. 1 A and Video 2 A). During this second phase, which started 1–3 min after the sealed phagosomes detached from the plasma membrane, actin transiently surrounded the entire phagosome and then dissociated asymmetrically, resulting in the appearance of an actin "comet tail" that drove short-lived phagosome displacement (Fig. 1 A and Video 2 B). Similar tails were also associated with phagosomes containing a variety of serum-coated targets, including *Yersinia pseudotuberculosis* (Fig. 1 B, top), zymosan (Fig. 1 B, bottom), live *Saccharomyces cerevisiae* (Video 3 A), and *Escherichia coli* (Video 3 B), that also activate CR3. Such cycles of actin polymerization and formation of actin tails were virtually absent during FcγR-mediated phagocytosis even when the cells were pretreated with PMA, which is routinely used for activation of CR3 (Fig. 1, C and D), suggesting these events were particular to CR3-mediated uptake.

Formation of actin tails requires Rac1

To assess the involvement of GTPases in the second wave of actin polymerization promoted by CR3, we used p21-binding domain (PBD)–PAK1–YFP, a fluorescent reporter of Rac1 and Cdc42 activity consisting of the PBD of PAK1 fused to YFP. A moderate but reproducible accumulation of PBD-PAK1–YFP was noted at sites of internalization, which disappeared shortly after phagosome closure (Fig. 1 E, Fig. S1, and Video 4), supporting a role for Rac and/or Cdc42 in CR3-mediated uptake. More strikingly, we detected the reassociation of the PBD-PAK1 around the phagosome shortly after sealing (Fig. 1 E). Coexpression of PBD-PAK1–YFP with mCherry-actin revealed that Rac and/or Cdc42 reactivation preceded and persisted through the second cycle of actin polymerization. Expression of Rac1–dominant negative (DN)–GFP suppressed the second cycle of actin polymerization, whereas DN Cdc42 had only a modest effect (Fig. 1 F). These observations suggest that, unlike the pathogen-induced comet tails, the actin tails formed by CR3 phagosomes are associated with and require Rho-family GTPase activation.

$PI(3,4)P_2$ and/or $PI(3,4,5)P_3$ accumulates on the phagosome during the second cycle of actin polymerization

In a variety of systems, $PI(3,4,5)P_3$ promotes and is often required for the activation of Rac/Cdc42 (Aoki et al., 2005). This phosphoinositide activates Rho-family guanine nucleotide exchange factors including Vav2, Vav3, and $PI(3,4,5)P_3$-dependent Rac exchanger (Welch et al., 2002; Aoki et al., 2005). We therefore investigated whether $PI(3,4,5)P_3$ mediates the activation of actin polymerization in sealed phagosomes. A fluorescent chimera containing the pleckstrin homology (PH) domain of the kinase Akt was used to monitor the distribution of 3′-polyphosphoinositides in cells engulfing C3bi-coated RBCs. Time-lapse microscopy indicated that, as reported earlier for FcγR-induced phagosomes (Marshall et al., 2001), PH-Akt–GFP accumulated on nascent CR3 phagosomes and dissociated shortly after sealing (Fig. 2 A and Video 5). Unlike FcγR phagosomes, however, CR3-induced phagosomes underwent one or more secondary waves of PH-Akt–GFP recruitment that coincided with the secondary cycles of actin polymerization (Fig. 2 A and Video 5). The probe associated uniformly around the phagosomal membrane even though actin became gradually polarized (Video 5). To ensure that these secondary waves were not caused by fluctuations in the focal plane, we labeled C3bi-coated RBCs with a fluorescent $F(ab')_2$ to track the location of the phagosomes (Fig. 2 B, insets). The intensities of PH-Akt–GFP and mCherry-actin clearly oscillated even when the constancy of the optical plane was verified, validating the occurrence of fluctuations in 3′-polyphosphoinositide content and ruling out optical artifacts (Fig. 2 C).

To examine the functional relationship between the formation of 3′-phosphoinositides and the polymerization of actin, we treated cells with wortmannin, an inhibitor of PI3K. Because formation of 3′-polyphosphoinositides by class I PI3K is required for the ingestion of large particles such as RBCs (Araki et al., 1996), the inhibitor was added immediately after phagocytosis was completed. Strikingly, wortmannin prevented PH-Akt association with formed phagosomes and completely abolished the formation of actin tails (Fig. 2, D and E). These observations imply that PI3K activity is required for the secondary wave of actin polymerization.

The PH domain of Akt recognizes not only $PI(3,4,5)P_3$ but also phosphatidylinositol-(3,4)-bisphosphate ($PI(3,4)P_2$). Because the probe associates with both inositides with similar affinity (Franke et al., 1997; Rong et al., 2001), we are unable to discern whether $PI(3,4)P_2$ or $PI(3,4,5)P_3$ is formed by the phagosomes. To better assess the presence of $PI(3,4,5)P_3$, we used a more selective probe. Macrophages were transfected with a fluorescent chimera encoding the PH domain of Gab2 (Gu et al., 2003), which preferentially binds $PI(3,4,5)P_3$. GFP–Gab2-PH

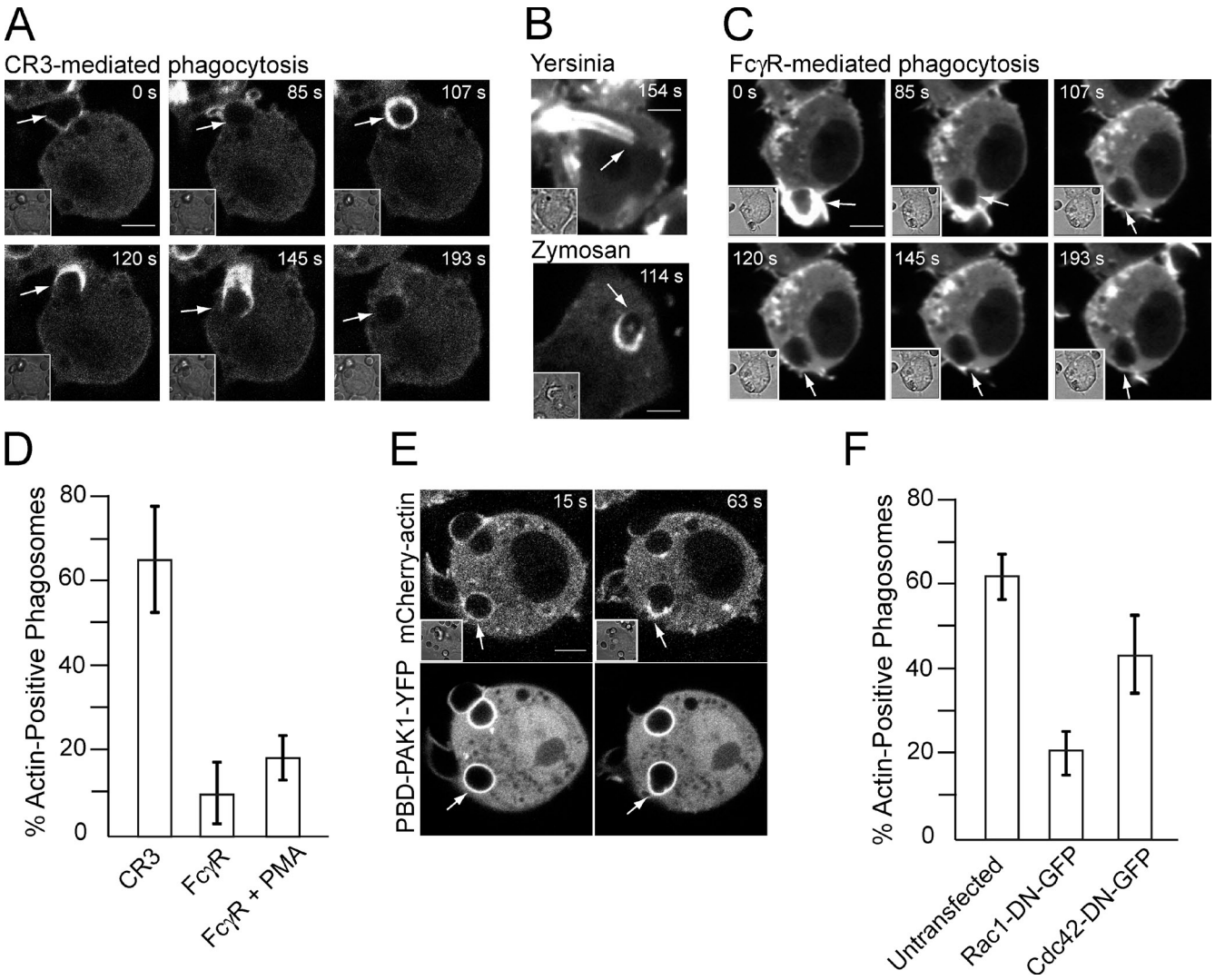

Figure 1. **Actin tails propel phagosomes after CR3-mediated phagocytosis.** (A–C and E) RAW264.7 macrophages stably expressing GFP-actin (A and C) or mCherry-actin (B and E) were examined by confocal microscopy after exposure to complement-coated RBCs (A and E), serum-coated *Y. pseudotuberculosis* or serum-coated zymosan (B) to trigger CR3-mediated phagocytosis, or IgG-coated RBCs (C) to trigger FcγR-mediated phagocytosis. (D) Quantitation of the percentage of phagosomes that displayed actin tails during the first 15 min after uptake. Data are means ± SEM of at least six individual experiments; a minimum of 70 phagosomes were counted per experiment. (E) PBD-PAK1–YFP was transfected transiently, and its dynamics were monitored in parallel with that of mCherry-actin. (F) Quantitation of the percentage of phagosomes that displayed actin tails during the first 15 min after uptake of complement-coated RBCs in cells transfected with DN forms of Rac1 or Cdc42. Data are means ± SEM of at least four individual experiments; a minimum of 60 phagosomes were counted per experiment. Images in A–C and E are representative of at least 10 individual experiments of each kind. Numbers indicate time in seconds after phagosome formation, and arrows point to the nascent or recently formed phagosomes. Insets illustrate corresponding differential interference contrast images. Bars, 5 µm.

associated with phagosomes during the second cycle of actin polymerization, whereas GFP–Gab2-PH(R32C), a mutant form lacking the ability to bind 3′-polyphosphoinositides, did not (Fig. S2), implying that $PI(3,4,5)P_3$ indeed accumulates in formed CR3-induced phagosomes.

$PI(4,5)P_2$ during the second cycle of actin polymerization

$PI(4,5)P_2$ has been implicated in several aspects of actin polymerization and remodeling, guiding the nucleation, elongation, and bundling of filaments (Hilpelä et al., 2004). Additionally, phosphorylation of $PI(4,5)P_2$ by class I PI3K is the main source of $PI(3,4,5)P_3$ (Hinchliffe, 2001), which we found to accumulate at the phagosome during the second wave of actin assembly. $PI(4,5)P_2$ is normally present on the membrane of unstimulated cells but, in the case of FcγR-induced phagocytosis, disappears during the course of particle engulfment as a result of degradation by phospholipase C and possibly also by phosphatases and is not detectable thereafter (Botelho et al., 2000). Because of the reformation of $PI(3,4,5)P_3$ and the reassembly of actin on the membrane of CR3 phagosomes, however, we anticipated the occurrence of a second wave of $PI(4,5)P_2$ in this system. This was tested in cells transfected with a GFP-tagged chimera of the PH domain of PLCδ. Contrary to our prediction, PH-PLCδ–GFP was not detectable in sealed CR3 phagosomes (Fig. 3 A, insets; and Video 6 A). It seemed conceivable that the PH-PLCδ–GFP probe lacked the sensitivity to detect a low yet significant concentration of $PI(4,5)P_2$. To enhance the sensitivity of our

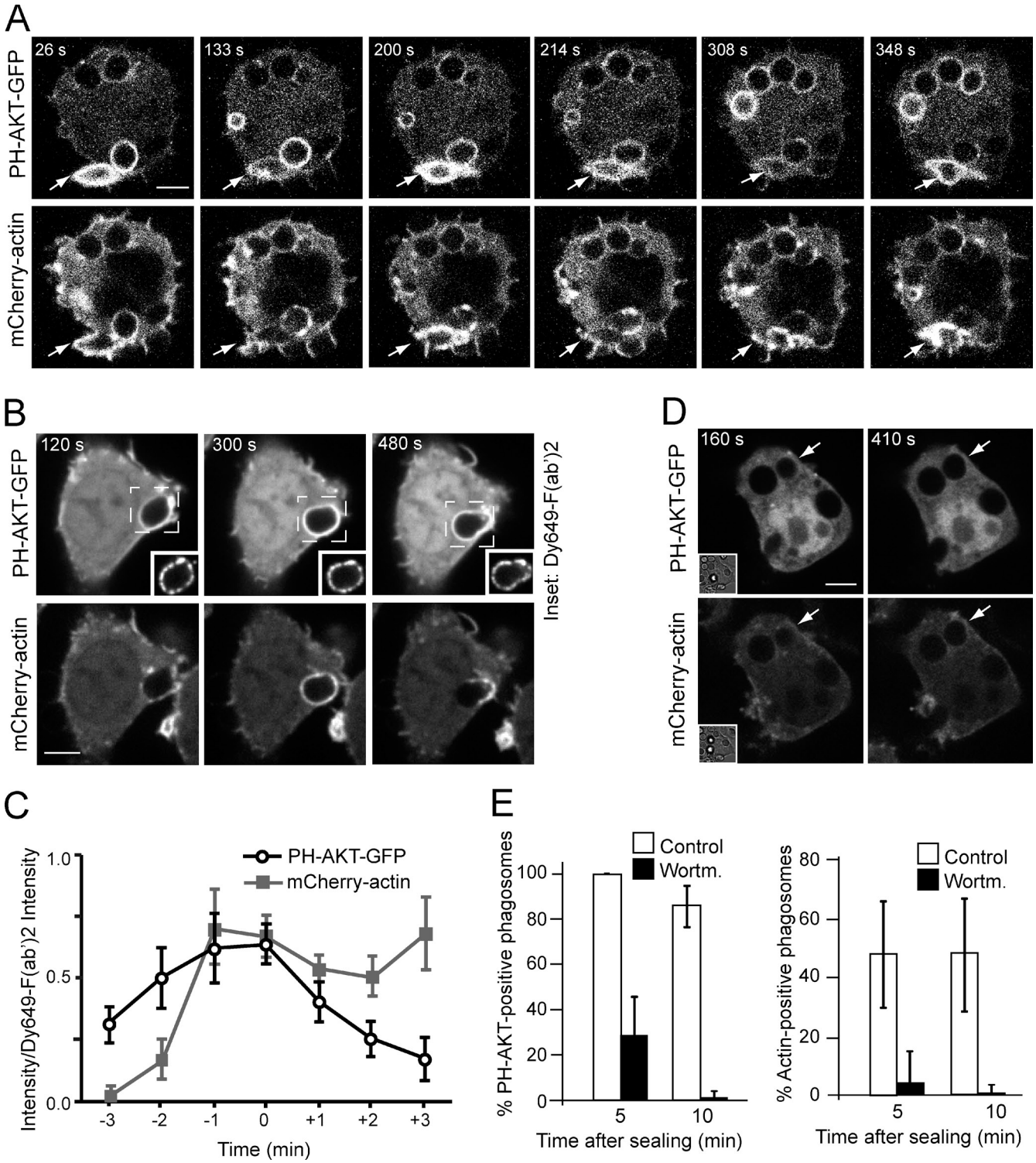

Figure 2. **PI(3,4)P_2/PI(3,4,5)P_3 accumulation in sealed phagosomes: role in actin tail formation.** (A, B, and D) RAW macrophages stably expressing mCherry-actin were transfected with PH-Akt–GFP and monitored after CR3-mediated uptake of complement-coated RBCs. In B, the complement-coated RBCs were marked with a fluorescent F(ab')$_2$ (insets) to verify the constancy of the focal plane. (C) Plots of the background-subtracted intensities of PH-Akt–GFP and mCherry-actin as ratios of the F(ab')$_2$ intensity ± SEM of 29 individual phagosomes. To control for the heterogeneous timing of PI(3,4,5)P_3 formation and actin tail formation after internalization, the plots were centered at time 0, which represents the moment of maximal PH-Akt–GFP recruitment to an internalized phagosome. (D) The cells were treated with 100 nM wortmannin immediately after phagocytosis was completed. Numbers indicate time in seconds after formation of phagosomes indicated by arrows. Insets illustrate corresponding differential contrast images. Images in A, B, and D are representative of at least six individual experiments of each kind. Bars, 5 µm. (E) Quantitation of PH-Akt– (left) or actin-positive phagosomes (right) at the indicated times after sealing. The cells were treated with 100 nM wortmannin shortly after phagocytosis was completed. Neither PH-Akt–GFP nor actin were detectable in wortmannin-treated samples after 10 min. Data, expressed as percentages, are means ± SEM of at least five individual experiments of each type; ≥80 phagosomes were counted per experiment.

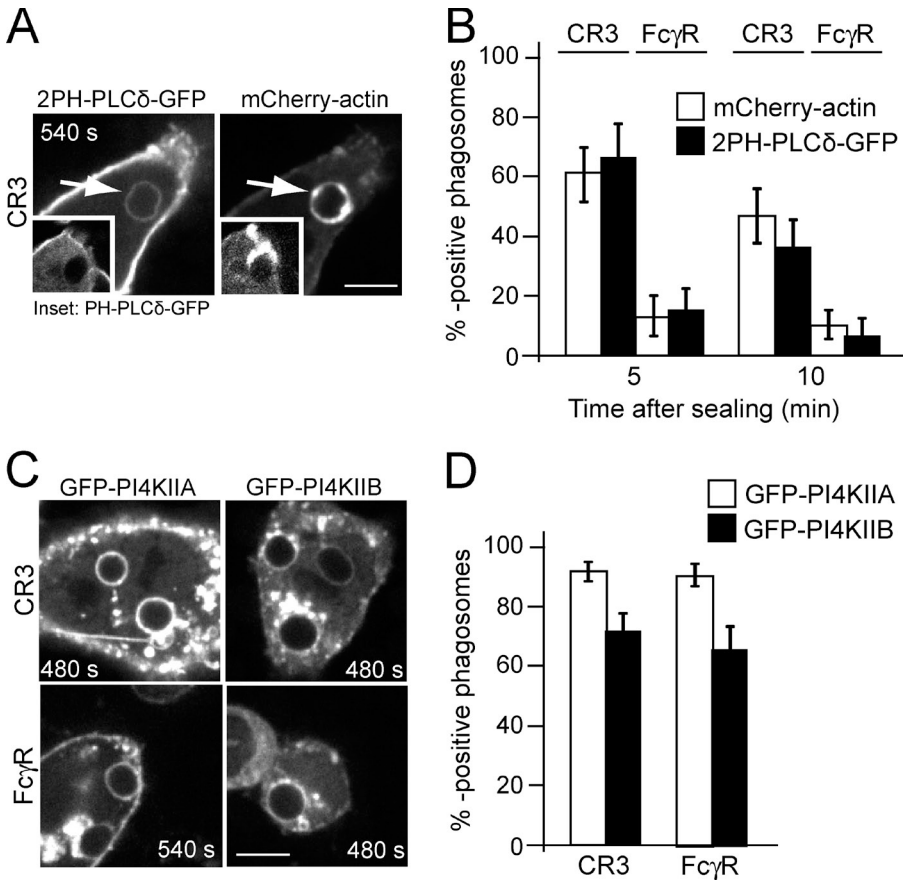

Figure 3. **Distribution of PI(4,5)P_2 and PI4KII during actin tail formation.** (A and C) Macrophages expressing the indicated constructs were analyzed by confocal microscopy after uptake of complement- or IgG-coated RBCs. Bars, 5 µm. (A) Cells stably expressing mCherry-actin (right) were transiently transfected with tandem 2PH-PLCδ–GFP (left). The insets show cells stably expressing mCherry-actin (right) transiently transfected with the single PH-PLCδ–GFP (left). (B) Quantitation of 2PH-PLCδ–GFP- and actin-positive phagosomes at the indicated times after sealing for both CR3- and FcγR-mediated phagocytosis. (C) Cells were transiently transfected with GFP-PI4KIIA (left) or GFP-PI4KIIB (right) and monitored after CR3- (top) or FcγR-mediated phagocytosis (bottom). (D) Quantitation of PI4KIIA- and PI4KIIB-positive phagosomes during the first 15 min after uptake of complement- and IgG-coated RBCs. Numbers indicate time in seconds after phagosome formation, and arrows point to the nascent or recently formed phagosome. Data, expressed as percentages, are means ± SEM of at least three individual experiments of each type; ≥50 phagosomes were counted per experiment.

assay, we transfected cells with a probe consisting of two tandem PH domains of PLCδ (2PH-PLCδ–GFP). This more sensitive probe (Mason et al., 2007) was detected on actin-positive CR3 phagosomes, albeit at a much lower level than at the plasma membrane (Fig. 3 A and Video 6 B). Of note, CR3 phagosomes were much more likely to retain 2PH-PLCδ–GFP than FcγR phagosomes (Fig. 2 B).

The de novo synthesis of PI(4,5)P_2 requires a supply of its precursor, phosphatidylinositol-(4)-phosphate (PI(4)P), generated by phosphatidylinositol 4-kinases (PI4Ks). As reported for phagosomes formed by *Listeria monocytogenes* in epithelial cells (Pizarro-Cerdá et al., 2007), we detected both PI4KIIA and PI4KIIB in phagosomes induced by CR3 and FcγR (Fig. 3, C and D).

Type I PI(4)P 5-kinase (PIP5K) is present at the phagosomal membrane during actin tail formation

Although phagosomes induced by either FcγR or CR3 accumulate PI4KII, only the latter proceed to generate PI(4,5)P_2 and PI(3,4,5)P_3 and form actin tails. This suggests that CR3 phagosomes possess a unique process for the conversion of PI(4)P to the more highly phosphorylated phosphoinositides. The mechanism used by CR3 phagosomes to generate PI(4,5)P_2 was investigated next. We analyzed the role of PIP5Ks, the enzymes responsible for the synthesis of PI(4,5)P_2 from PI(4)P (Loijens et al., 1996). Macrophages were transfected with GFP-tagged versions of the main PIP5KI isoforms. As reported for FcγR phagocytosis (Fairn et al., 2009), we found that overexpression of the kinases reduced phagocytic efficiency of CR3-coated RBCs, an effect that was most pronounced for PIP5KIα; we therefore studied primarily the fate of PIP5KIβ and PIP5KIγ. Both kinases were abundant at the plasma membrane and accumulated at the phagocytic cup during both FcγR- and CR3-mediated phagocytosis (see Fig. 4 for an illustration of PIP5KIγ). As shown previously (Botelho et al., 2000; Coppolino et al., 2002), in the case of FcγR-mediated uptake, the accumulation of PIP5KI was transient; the enzyme detached from the phagosomes upon sealing and was not seen to reassociate thereafter (Fig. 4 B). In sharp contrast, both PIP5KIβ and PIP5KIγ remained associated with CR3-induced phagosomes for ≥10–15 min after the phagosomes sealed (Fig. 4, A and C). Indeed, the kinases persisted on the phagosomal membrane at the time when PI(3,4,5)P_3 formed and actin accumulated around the phagosome (Fig. 4 D).

Recruiting PIP5KI to FcγR phagosomes induces a second wave of PI(4,5)P_2 and PI(3,4,5)P_3 accumulation and actin polymerization

The persistence of PIP5KI at the phagosome after CR3- but not FcγR-mediated uptake, as well as its coincidence with the second cycle of actin polymerization, suggests that PIP5KI is the enzyme responsible for the synthesis of PI(4,5)P_2 from PI(4)P. Because PIP5KI activity is strictly necessary during the initial stages of phagocytosis, it was impossible to test the role of this

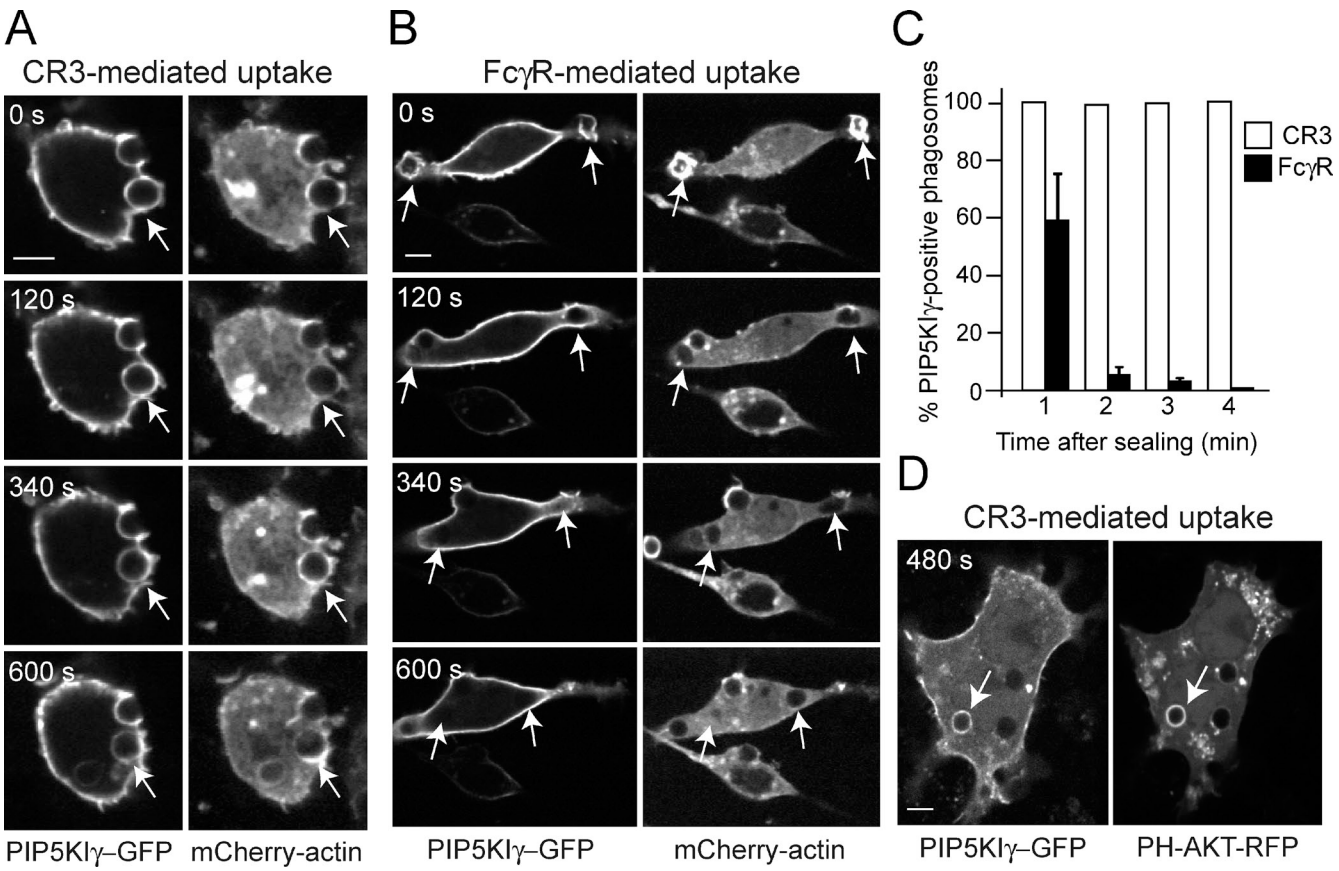

Figure 4. **PIP5KI dynamics during CR3- and FcγR-mediated phagocytosis.** (A and B) Macrophages stably expressing mCherry-actin were transiently transfected with PIP5KIγ-GFP and examined by confocal microscopy after exposure to complement- (A) or IgG-coated RBCs (B). The images are representative of seven experiments. Bars, 5 µm. (C) Quantification of PIP5KIγ-GFP–positive phagosomes at the indicated times after sealing for both CR3- and FcγR-mediated phagocytosis. Data, expressed as percentages, are means ± SEM of at least four individual experiments of each type; ≥20 phagosomes were counted per experiment. (D) Colocalization of PIP5KIγ-GFP with PH-Akt–RFP during CR3-mediated phagocytosis. Numbers indicate time in seconds after phagosome formation, and arrows point to the nascent or recently formed phagosomes.

kinase by expression of DN constructs, which prevent phagocytosis (Coppolino et al., 2002). Gene silencing using siRNA would be subject to the same limitations and complicated by the existence of multiple, potentially redundant PIP5KI isoforms. Instead, we used a gain-of-function approach, inducing the retention of PIP5KI on FcγR-generated phagosomes, which normally fail to retain the kinase and do not display secondary waves of actin association. This was accomplished using an inducible, rapamycin-mediated heterodimerization system (Inoue et al., 2005). The system consists of two components: a rapamycin-binding domain coupled to the short splice variant of PIP5KIγ fused to a fluorescent marker (YFP–FK506-binding protein [FKBP]–PIP5K) and a second rapamycin-binding moiety fused to the membrane-targeting N-terminal sequence of Lyn (Lyn11-directed rapamycin-binding domain [LDR]; Fig. 5). In the absence of rapamycin, YFP–FKBP-PIP5K is largely soluble, and no association with sealed phagosomes is detectable (Fig. 5 B). Under these conditions, as in untransfected cells, no PH-PLCδ–RFP—indicative of $PI(4,5)P_2$—associates with fully formed FcγR phagosomes. Upon addition of rapamycin, however, YFP–FKBP-PIP5K is recruited to the plasma membrane and also to recently formed phagosomes, where LDR resides (Fig. 5 B and Video 7). In nearly all phagosomes, recruitment of PIP5KI was associated with accumulation of PH-PLCδ–RFP (Fig. 5 B). The level of PH-PLCδ–RFP at the plasmalemma remained unchanged.

As in untransfected cells, the FcγR phagosomes were mostly devoid of mCherry-actin in cells coexpressing YFP–FKBP-PIP5K and LDR. Adding rapamycin induced the polymerization of actin and the formation of robust comet tails (Fig. 5, D and G; Fig. S3 D; and Video 8). The addition of rapamycin to untransfected cells or to cells expressing LDR plus a chimera of FKBP and YFP lacking PIP5K had no effect on actin polymerization (Fig. 5 G, Fig. S3 E, and Video 9). Addition of rapamycin to cells expressing LDR plus a chimera of FKBP and CFP containing a kinase-dead version of PIP5K produced a small yet significant degree of actin polymerization (Fig. 5 G). The mechanism underlying this modest activation of actin remains unclear, but heterodimerization of endogenous wild-type enzyme with the kinase-dead mutant is a distinct possibility.

Two lines of evidence indicate that formation of $PI(3,4,5)P_3$ was responsible for the polymerization of actin promoted by recruitment of PIP5KI. First, the addition of rapamycin to cells coexpressing YFP–FKBP-PIP5K and LDR (Fig. 5 C, inset) induced the recruitment of PH-Akt–RFP, indicative of $PI(3,4)P_2$/$PI(3,4,5)P_3$, to the phagosomal membrane (Fig. 5, C and G; and

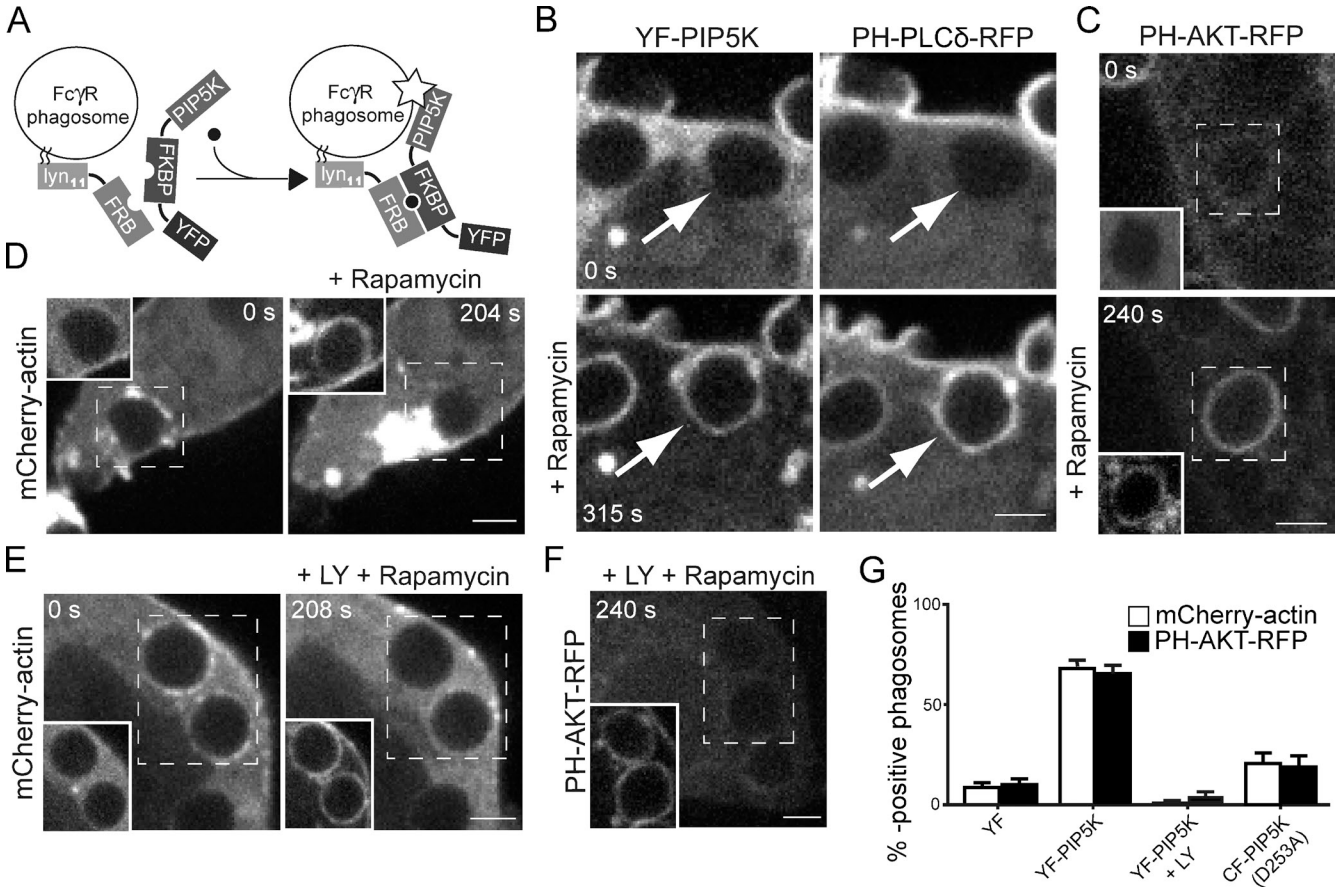

Figure 5. **Rapamycin-induced recruitment of PIP5KI during FcγR-mediated phagocytosis.** (A) Experimental strategy: RAW macrophages were transfected with two complementary rapamycin-binding domains (LDR, which includes the membrane-targeting N-terminal sequence of Lyn and either PIP5KIγ-FKBP–YFP [YF-PIP5K] or FKBP-YFP [YF]). Addition of rapamycin (black dot) after FcγR-mediated phagocytosis of IgG-coated RBCs induces translocation of the FKBP domain-containing constructs to the phagosome. The star indicates PIP5K activity on the phagosomal membrane. (B) PH-PLCδ–RFP, PIP5KIγ-FKBP–YFP, and LDR were coexpressed transiently, and phagocytosis of IgG-coated RBCs was initiated. Images acquired immediately before (top) and 315 s after addition of 1 μM rapamycin are shown. Arrows point to the nascent or recently formed phagosomes. (C) PH-Akt–RFP, PIP5KIγ-FKBP–YFP, and LDR were coexpressed transiently, and phagocytosis was initiated as in B. Images were acquired 240 s after addition of rapamycin. (D) PIP5KIγ-FKBP–YFP and LDR were coexpressed transiently in RAW cells stably expressing mCherry-actin, and phagocytosis of IgG-coated RBCs was initiated. Images of mCherry-actin acquired immediately before (left) and 204 s after addition of 1 μM rapamycin are shown in the main panels. (E) PIP5KIγ-FKBP–YFP and LDR were coexpressed transiently in RAW cells stably expressing mCherry-actin, and phagocytosis of IgG-coated RBCs was initiated. Shortly after ingestion, the cells were treated with 100 μM LY294002 and then with 1 μM rapamycin. Images acquired 208 s after addition of rapamycin are shown. (F) PH-Akt–RFP, PIP5KIγ-FKBP–YFP, and LDR were coexpressed transiently. Shortly after ingestion, the cells were treated with 100 μM LY294002 and then with rapamycin. Images of mCherry-actin acquired 240 s after addition of rapamycin are shown in the main panels. In C–F, the insets show the distribution of PIP5KIγ-FKBP–YFP before (0 s) and at the indicated times after addition of rapamycin. Images in B–F are representative of five separate experiments, each analyzing ≥40 phagosomes. Bars, 3 μm. (G) Quantification of multiple experiments like those in C–F. Data are means ± SEM of five separate experiments.

Fig. S3 A). It is noteworthy that in the same experiments PH-Akt–RFP was not recruited to the plasma membrane (Fig. 5 C), suggesting that the pertinent 3′-kinase is inactive or absent at the plasmalemma and functions only on the phagosomal membrane. Accordingly, the rapamycin-induced binding of PH-Akt–RFP to phagosomes was obliterated by LY294002, a PI3K inhibitor (Fig. 5, F and G; and Fig. S3 C). LY294002 also provided evidence that $PI(3,4)P_2/PI(3,4,5)P_3$ was responsible for the polymerization of actin observed upon recruitment of PIP5KI to FcγR phagosomes. The PI3K inhibitor eliminated the association of actin and the formation of comet tails induced by rapamycin (Fig. 5, E and G; and Fig. S3 F). By recapitulating in FcγR phagosomes the PIP5KI-induced formation of $PI(4,5)P_2$ and $PI(3,4)P_2/PI(3,4,5)P_3$ and the second wave of actin polymerization, these experiments provide indirect evidence for the role of PIP5KI during CR3-mediated phagocytosis.

Class I PI3K accumulates on phagosomes

Although the recruitment of PIP5KI is sufficient to produce $PI(4,5)P_2$ on maturing phagosomes, a 3′-kinase is required for the conversion of $PI(4,5)P_2$ into $PI(3,4,5)P_3$. The observed inhibitory effects of LY294002 and wortmannin on the accumulation of PH-Akt support this notion. Class I PI3Ks normally underlie the formation of $PI(3,4,5)P_3$ from $PI(4,5)P_2$ at the plasma membrane but have not been reported to act in endomembranes. To assess their involvement, we first studied their distribution during phagocytosis. To visualize class I PI3K, we used the regulatory subunit of class PI3K, p85, fused to YFP. In unstimulated cells, this chimera was largely soluble and absent from the plasmalemma (Fig. 6 B), consistent with the failure of PH-Akt to accumulate at the plasmalemma after PIP5K recruitment (Fig. 5 C). During CR3-induced phagosome formation, p85 accumulated at the phagosomal cup, and, after sealing, the kinase was retained by

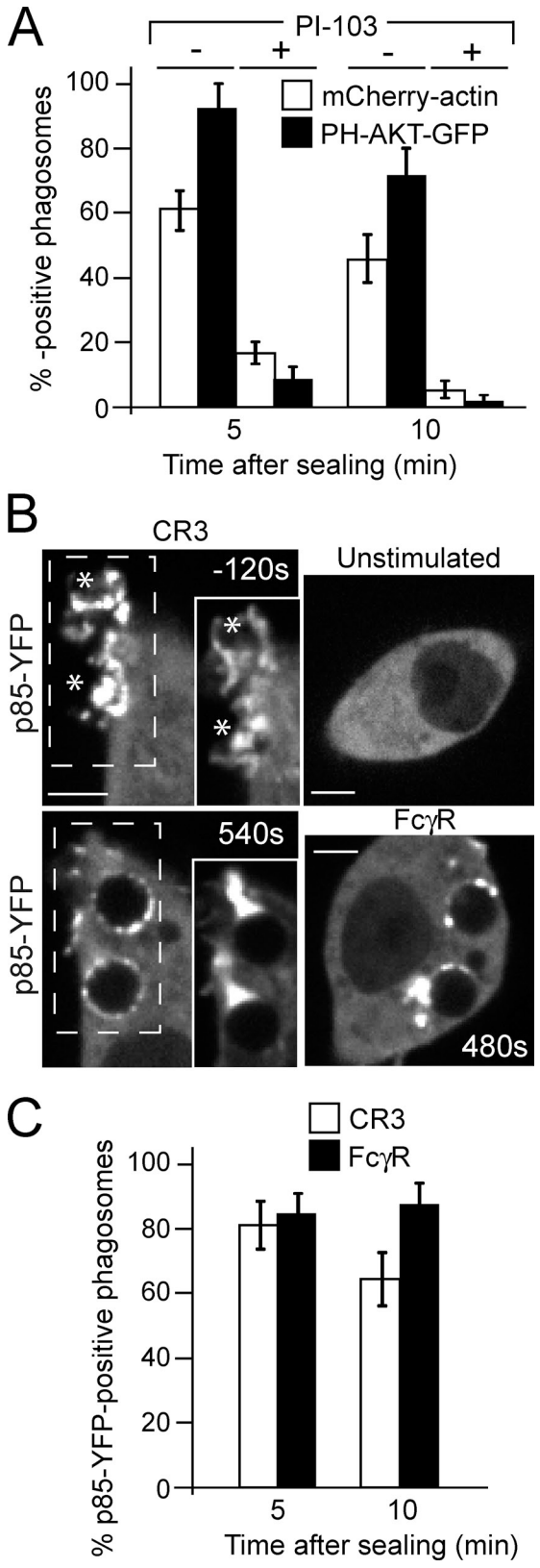

Figure 6. **Role of PI3KI during actin tail formation.** (A) Macrophages stably expressing mCherry-actin were transiently transfected with PH-Akt–GFP, and phagocytosis of complement-coated RBCs was initiated. Shortly after ingestion, the indicated cells were treated with 100 nM PI-103. The percentage of phagosomes that were actin or PH-Akt positive was quantified at the indicated times after sealing. (B) Macrophages stably expressing mCherry-actin were transiently transfected with p85-YFP. Cells were left unstimulated (top right) or made to ingest complement- (left) and IgG-coated RBCs (bottom right). Main panels show p85-YFP, and, where present, insets show mCherry-actin. Asterisks indicate forming phagosomes. Bars, 3 µm. (C) Quantitation of the percentage of p85-YFP–positive phagosomes at the indicated times after sealing for both CR3- and FcγR-mediated phagocytosis. Data, expressed as percentages, are means ± SEM of at least three individual experiments of each type; ≥40 phagosomes were counted per experiment.

phagosomes for significant periods of time, overlapping with the actin polymerization stage (Fig. 6, B and C). A punctate pattern of p85 was also seen around phagosomes induced by FcγR (Fig. 6 B) despite the fact they failed to accumulate $PI(3,4,5)P_3$ or actin. These observations suggest that class I PI3K may be responsible for $PI(3,4,5)P_3$ generation in CR3 phagosomes, which retain PIP5KI and can therefore generate $PI(4,5)P_2$, and that failure of FcγR phagosomes to make $PI(3,4,5)P_3$ is attributable to the absence of PIP5KI and not class I PI3K.

LY294002 and wortmannin inhibit not only class I PI3K but also the class III Vps34 that is active in phagosomes. The latter could in principle also contribute to $PI(3,4,5)P_3$ formation because its product, PI(3)P, functions in vitro as a substrate for the formation of $PI(3,4)P_2$/$PI(3,4,5)P_3$ by PIP5KI (Zhang et al., 1997). To discern the contributions of the two types of kinases, we used PI-103, an inhibitor that when used in the nanomolar range inhibits class I PI3K but not class III (Fan et al., 2006). At 100 nM, PI-103 inhibited phagocytosis—a class I–dependent process—by >80% (not depicted) and did not affect PI(3)P formation (Video 10). To assess its effects on $PI(3,4,5)P_3$ and actin accumulation on sealed phagosomes, we added the drug 2 min after particle ingestion was completed. Strikingly, PI-103 prevented PH-Akt association with formed phagosomes and completely abolished the formation of actin tails (Fig. 6 A). These observations imply that class I PI3K activity is required for $PI(3,4,5)P_3$ formation and for the secondary wave of actin polymerization.

The second wave of actin polymerization depends on PI(3)P

The inhibition of actin tail formation by PI-103 establishes the role of class I PI3K but does not preclude the possibility that class III PI3K may also be involved in the process. After FcγR-mediated phagocytosis, PI(3)P appears on the phagosomal membrane shortly after closure (Vieira, et al., 2001), directing fusion with late endosomes and lysosomes. That PI(3)P is also generated in the course of CR3-induced phagocytosis was verified using a construct consisting of two tandem FYVE domains of EEA1 tagged with GFP. As illustrated in Fig. 7 A, PI(3)P was routinely found to appear on CR3 phagosomes shortly after sealing, where it persisted for ∼10 min, recapitulating the observations in FcγR phagosomes (Vieira et al., 2001). As anticipated, 2FYVE-GFP recruitment was obliterated by wortmannin (Fig. 7 B).

Because PI(3)P formation coincided and often preceded the association of actin with the sealed phagosome (Fig. 7 A), we considered the possibility that it may regulate the de novo formation of $PI(4,5)P_2$ and $PI(3,4,5)P_3$. To further analyze the PI(3)P dependence of actin tail formation, and because selective

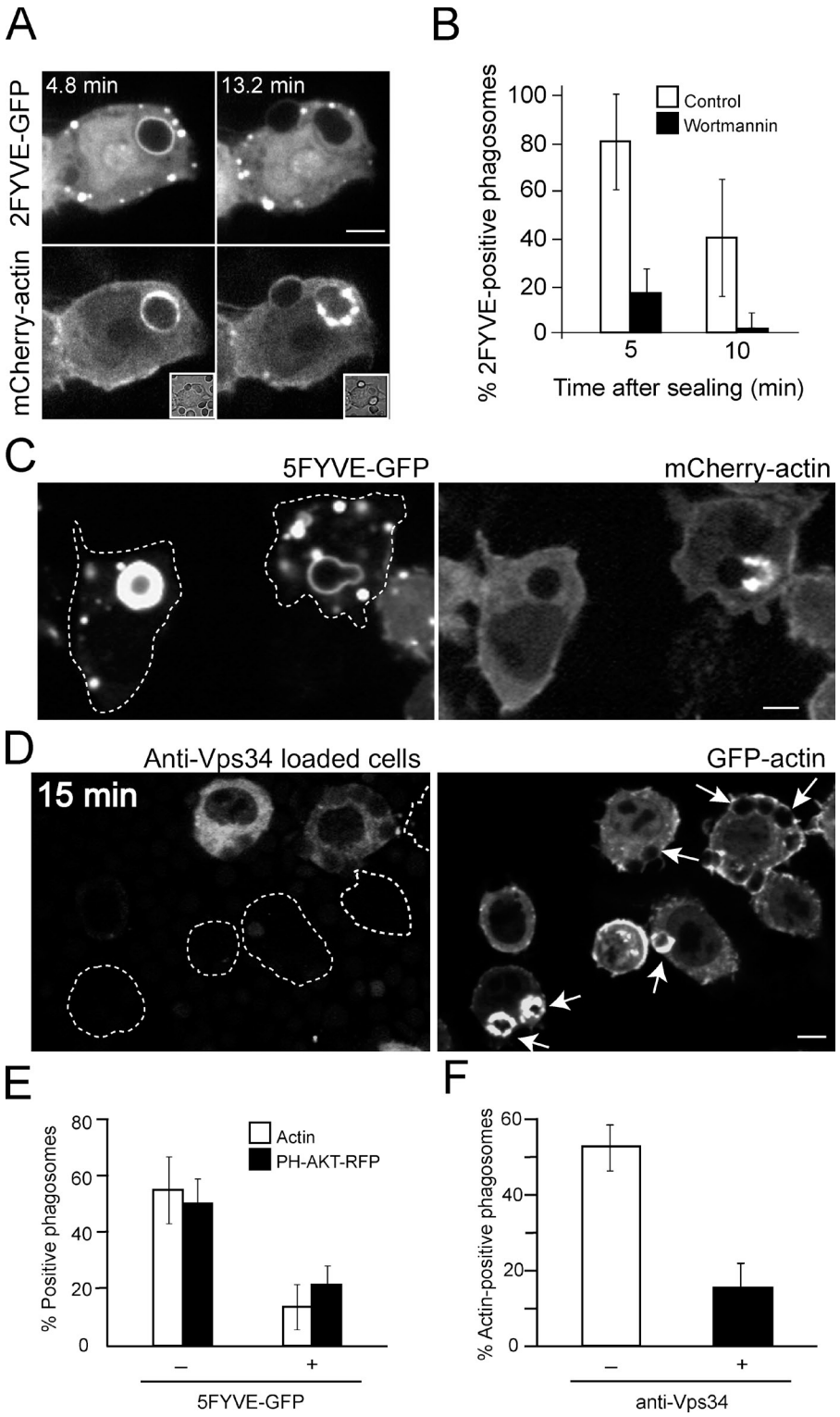

Figure 7. **PI(3)P is required for actin tail formation.** Macrophages expressing the indicated constructs were analyzed by confocal microscopy after CR3-mediated uptake of complement-coated RBCs. Insets show corresponding differential interference contrast images. Numbers indicate time after phagosome formation. Bars, 5 μm. (A) Cells stably expressing mCherry-actin (bottom) were transiently transfected with 2FYVE-GFP (top). (B) Quantitation of 2FYVE-positive phagosomes at the indicated times after sealing. The cells were treated with 100 nM wortmannin shortly after ingestion of the RBCs. Data, expressed as percentages, are means ± SEM of at least six individual experiments of each type; ≥70 phagosomes were counted per experiment. (C) Macrophages stably expressing mCherry-actin (right) were transiently transfected with a construct consisting of five tandem FYVE domains coupled to GFP (left). The dotted lines delineate the cell outlines on the left. (D) Macrophages stably expressing GFP-actin (right) were loaded with anti-Vps34 antibody in the presence of rhodamine-conjugated dextran (left), which was used to identify the cells that were transiently permeabilized by the bead-loading procedure. The dotted lines delineate the outlines of unloaded cells displaying actin-labeled phagosomes. Arrows point to the nascent or recently formed phagosomes. Images in A, C, and D are representative of at least four individual experiments. (E) Quantification of actin- or PH-Akt–RFP-positive phagosomes in cells transiently transfected with 5FYVE-GFP. (F) Quantification of actin-positive phagosomes in cells loaded with an anti-Vps34 antibody (+) or subjected to the permeabilization protocol and either unloaded or loaded with an irrelevant antibody. Data in E and F are means ± SEM of at least four individual experiments; ≥25 phagosomes were counted per experiment.

inhibitors of class III PI3K are not available, we instead attempted to sequester the phosphoinositide by overexpressing a construct consisting of five tandem FYVE domains. Because of the high avidity conferred by multiple conjoined FYVE domains, this GFP-tagged chimera is predicted to effectively scavenge PI(3)P, precluding access by proteins that depend on its signaling. As shown in Fig. 7 (C and E), formation of $PI(3,4,5)P_3$ and recruitment of actin around CR3 phagosomes were absent in cells that expressed high levels of 5FYVE-GFP but not in cells with low expression levels.

We also inhibited the class III PI3K selectively by loading the macrophages with neutralizing anti-Vps34 antibodies. Cells were transiently permeabilized using glass beads in the presence of concentrated antibody and rhodamine-labeled dextran, which was used to identify the loaded cells. Antibody-loaded cells showed a marked inhibition of actin tail formation compared

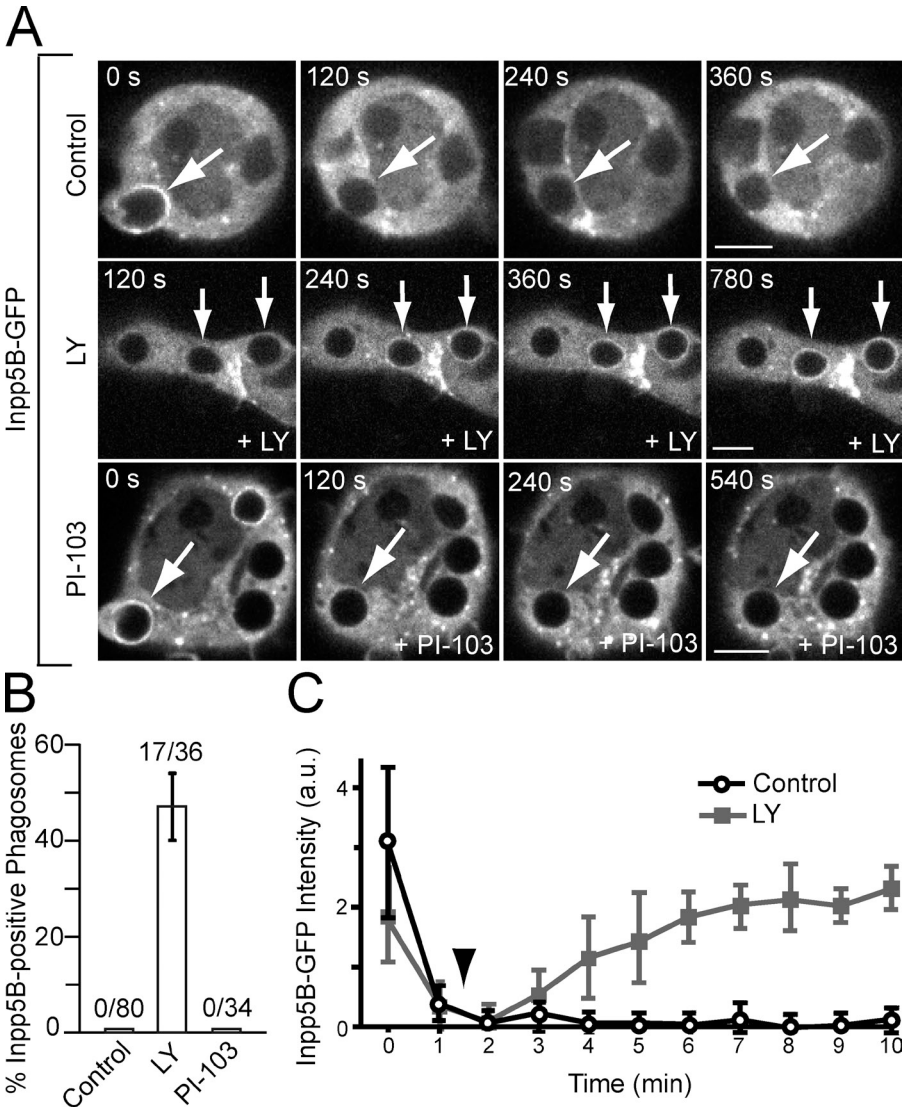

Figure 8. **PI(3)P controls the association of Inpp5B with phagosomes.** (A) Cells were transiently transfected with Inpp5B-GFP, and phagocytosis of complement-coated RBCs was initiated. Shortly after ingestion of the RBCs, the cells were treated with 100 µM LY294002 (middle) or 100 nM PI-103 (bottom). Numbers indicate time in seconds after phagosome formation, and arrows point to the nascent or recently formed phagosomes. Bars, 5 µm. (B) Quantitation of the percentage of phagosomes that was Inpp5B-GFP positive at 10 min after phagosome sealing. Data are means ± SEM of at least three individual experiments; ≥30 phagosomes were counted. The numbers indicate the fraction of Inpp5B-positive phagosomes. (C) Plots of the background-subtracted intensity of Inpp5B-GFP for phagosomes under control conditions and when 100 µM LY294002 (arrowhead) was added shortly after phagosome closure (squares). Data are means ± SEM of at least three individual experiments; ≥10 phagosomes were counted per experiment. a.u., arbitrary units.

with control cells (Fig. 7, D and F). The ability of loaded cells to ingest particles indicates that the loading procedure did not cause irreversible damage, nor did it impair the ability of the cells to polymerize actin, a necessary requirement for bead engulfment. Indeed, cells subjected to the bead-loading protocol that did not take up antibody or that were loaded with an irrelevant antibody showed near-normal levels of actin polymerization around CR3 phagosomes (Fig. 7 D). Jointly, these observations indicate that PI(3)P formed by class III PI3K is also required for actin tail formation.

PI(3)P displaces Inpp5B, an inositol 5-phosphatase

How does PI(3)P contribute to PI(3,4,5)P_3 accumulation and actin polymerization? Several mechanisms can be envisaged: PI(3)P may be required to retain or activate class I PI3K, to preclude the action of polyphosphoinositide phosphatases, or to recruit additional effectors.

We found that, despite treatment with LY294002, class I PI3K (assessed monitoring p85) was recruited and retained by sealed CR3 phagosomes (unpublished data). We therefore proceeded to analyze the possible role of phosphatases. Inpp5B is an inositol 5-phosphatase that preferentially dephosphorylates the 5′ position of PI(4,5)P_2 and PI(3,4,5)P_3 (Erdmann et al., 2007). Interestingly, Inpp5B binds to APPL1, a protein that accumulates in endosomes and macropinosomes when PI(3)P is depleted (Zoncu et al., 2009). We therefore considered the possibility that class III PI3K controls the level of PI(3,4,5)P_3 in phagosomes by dictating the association/dissociation of Inpp5. As illustrated in Fig. 8 (A and C), Inpp5B-GFP was recruited to forming phagosomes but dissociated shortly after sealing, failing to reassociate thereafter, mirroring the dynamics of its binding partner, APPL1 (Fig. S4).

Remarkably, treatment of the cells with LY294002 immediately after phagocytosis caused a striking reaccumulation of Inpp5B that lasted up to 30 min (Fig. 8, A–C). The reaccumulation induced by LY294002 was, in all likelihood, caused by inhibition of class III PI3K and not class I because the effect was not replicated by PI-103 (Fig. 8, A and B). Jointly, these results suggest that formation of PI(3)P, the product of class III PI3K, is required for the dissociation of Inpp5, which enables the accumulation of PI(4,5)P_2, PI(3,4,5)P_3, and actin on sealed phagosomes.

Actin tails accelerate CR3 phagosome maturation

The functional significance of actin tail formation was explored next. Sealed phagosomes undergo a series of fusion and fission events collectively called maturation that convert them into phagolysosomes, hybrid organelles with enhanced microbicidal capacity. We considered whether formation of actin tails affects the rate of maturation, perhaps by bringing phagosomes in close proximity to endocytic subcompartments. Macrophages were challenged with C3bi-coated RBCs for 5 min and then incubated with a fluorescent $F(ab')_2$ to label uninternalized RBCs, allowing assessment of maturation in adequately synchronized phagosomes. Phagosomal maturation was analyzed at different times in cells treated with or without latrunculin B, an actin polymerization inhibitor, identifying mature phagolysosomes with LysoTracker. Treatment with latrunculin B reduced the rate and extent of phagolysosome formation (Fig. 9), suggesting that actin tail formation expedites phagosome maturation. However, other indirect effects of actin depolymerization cannot be discounted.

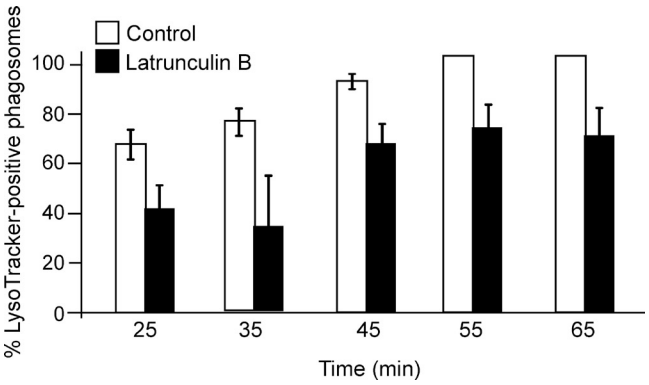

Figure 9. **Inhibition of actin tails delays maturation.** Cells were exposed to complement-coated RBCs. After 5 min, the cells were exposed to 10 µM latrunculin B, and uninternalized RBCs were labeled with a fluorescent $F(ab')_2$. At the indicated times after the addition of RBCs, LysoTracker was added, and cells were visualized by confocal microscopy. Data, expressed as the percentage of LysoTracker-positive phagosomes, are means ± SEM of at least three individual experiments. Each experiment included >10 phagosomes.

Discussion

The salient finding of these studies is that actin is recruited to sealed CR3 phagosomes by a process that requires the activity of class I PI3K as well as Vps34, the class III PI3K. However, the presence of class I and class III kinases on the phagosomal membrane is insufficient to induce actin polymerization; phagosomes induced by activation of FcγR display a consistent, robust accumulation of PI(3)P (Vieira et al., 2001) yet rarely recruit actin (Fig. 1; Choi et al., 2008). Our data indicate that actin assembly correlates instead with the formation of $PI(4,5)P_2$ and $PI(3,4,5)P_3$, which are detectable only in phagosomes generated by CR3 and not in those induced by FcγR. Actin does assemble onto FcγR phagosomes when $PI(4,5)P_2$/$PI(3,4,5)P_3$ formation is imposed by inducible recruitment of heterologously expressed kinases (Fig. 5).

In mammalian cells, $PI(3,4,5)P_3$ is thought to be generated primarily via phosphorylation of $PI(4,5)P_2$ by class I PI3K (Hinchliffe, 2001). $PI(3,4)P_2$ is formed by dephosphorylation of $PI(3,4,5)P_3$ catalyzed by 5′-phosphatases such as Src homology 2 domain–containing inositol 5-phosphatase. These reactions are likely to account for the appearance of $PI(3,4)P_2$ and $PI(3,4,5)P_3$ in CR3 phagosomes inasmuch as (a) $PI(4,5)P_2$ is detectable in their membranes, (b) p85 is present when they appear, and (c) PI-103 suppresses their formation. The class I kinase was also found on the membrane of FcγR phagosomes, yet these failed to generate $PI(3,4,5)P_3$. We attribute this difference to the absence of $PI(4,5)P_2$, the substrate of class I PI3K. Our data indicate that PIP5KI, the enzyme that generates $PI(4,5)P_2$, is in fact retained by CR3-induced phagosomes but not by those formed by FcγR, mirroring the appearance of $PI(3,4)P_2$ and $PI(3,4,5)P_3$ and the recruitment of actin. Validation of a causal relationship between these events by knockdown or pharmacological inhibition of PIP5KI is not feasible because phagocytosis depends on the activity of these enzymes. However, the ability of phagosomal PIP5KI to convert PI(4)P to $PI(4,5)P_2$ was demonstrated by inducing its recruitment with rapamycin to FcγR phagosomes, which are otherwise devoid of the kinase. Therefore, we conclude that CR3 phagosomes have the unique ability to synthesize $PI(3,4,5)P_3$ by retaining PIP5KI.

Not only was the activity of PIP5KI and class I PI3K required for accumulation of $PI(3,4,5)P_3$, but so was the activity of class III PI3K. Indeed, blocking the headgroups of PI(3)P or preventing its formation using inhibitory anti-Vps34 antibodies precluded $PI(3,4,5)P_3$ accumulation and actin rocketing. Our data suggest that PI(3)P acts by terminating the activity of Inpp5 (and possibly other phosphatases) on sealed phagosomes. Accordingly, although Inpp5 rapidly dissociated from CR3 phagosomes in untreated cells, it lingered at high concentrations for up to 30 min if PI(3)P formation was blocked. Preliminary data indicate that Inpp5 retention in this case is mediated by APPL1, which in turn binds to Rab5. We had shown earlier that the residence time of Rab5 in phagosomes is greatly extended when PI(3)P formation is impaired (Vieira et al., 2001). Thus, the activity of the class III PI3K is essential to dislodge the phosphatase, thereby allowing the accumulation of $PI(4,5)P_2$ and $PI(3,4,5)P_3$. The complex coordinated series of events that is required for $PI(3,4,5)P_3$ accumulation and actin tail formation and the differences between CR3 and FcγR phagosomes are illustrated diagrammatically in Fig. 10.

The absence of PIP5KI from FcγR phagosomes was recently attributed to changes in the surface charge of the phagosomal membrane, which were in turn associated with depletion of the polyanionic $PI(4,5)P_2$ (Fairn et al., 2009). Because $PI(4,5)P_2$ was found to be present on CR3 phagosomes, it could be the means for the retention of PIP5KI on their membrane. In this regard, the long variant of PIP5KIγ is also known to associate with talin (Ling et al., 2002), an adaptor protein that links integrins with the cytoskeleton. Because the complement receptor CR3 is a member of the integrin family, it is conceivable that PIP5KIγ is recruited to the phagosomes via talin. Of note, talin is detectable around phagosomes containing C3bi-opsonized RBCs and is in fact essential for CR3-mediated uptake (Lim et al., 2007). Therefore, retention of PIP5KIγ on the

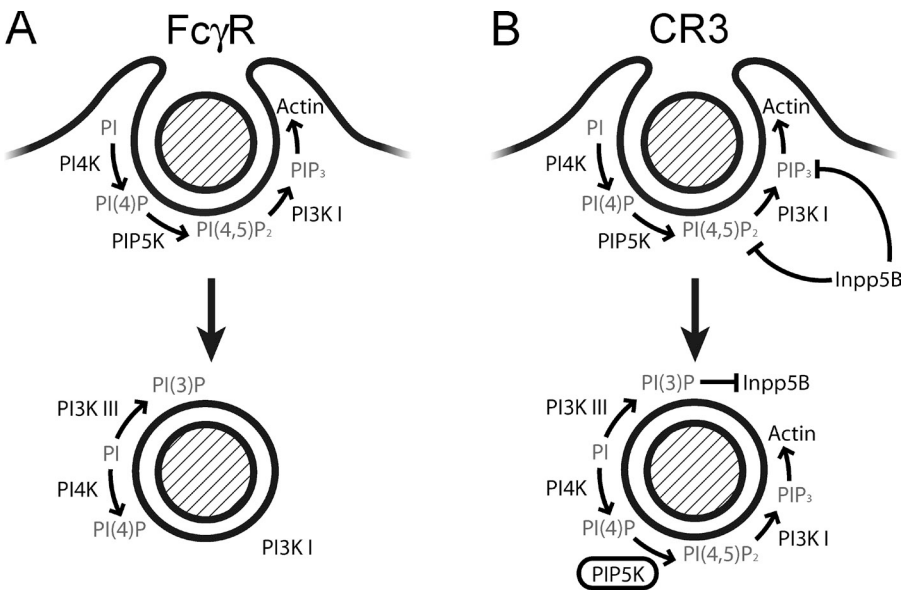

Figure 10. **Diagrammatic representation of phosphoinositide metabolism and actin recruitment.** (A) FcγR-mediated phagocytosis. (B) CR3-mediated phagocytosis. (A) During FcγR-mediated phagosome formation (top), phosphoinositide kinases transform phosphoinositide into $PI(4,5)P_2$ and $PI(3,4,5)P_3$ and regulate actin polymerization within the growing pseudopod. Although PI4K and PI3KI remain associated with the maturing FcγR-mediated phagosome (bottom), PIP5K detaches upon sealing, resulting in depletion of $PI(4,5)P_2$ and failure to accumulate $PI(3,4,5)P_3$. (B) CR3-mediated phagosome formation (top) mirrors FcγR-mediated phagosome formation in terms of $PI(4,5)P_2$ and $PI(3,4,5)P_3$ synthesis and actin polymerization. The 5′-phosphoinositide phosphatase Inpp5B likely contributes to hydrolyze $PI(4,5)P_2$ and $PI(3,4,5)P_3$ during phagosome sealing. Unlike FcγR-mediated phagosomes, CR3-mediated phagosomes (bottom) retain PIP5K after sealing, which allows de novo $PI(4,5)P_2$ and $PI(3,4,5)P_3$ synthesis and actin polymerization. Accumulation of $PI(4,5)P_2$ and $PI(3,4,5)P_3$ is possible because PI(3)P dislodges Inpp5B.

phagosomal membrane via CR3 by $PI(4,5)P_2$ and/or talin could explain the conversion of PI(4)P to $PI(4,5)P_2$. However, other means of attachment and the involvement of other isoforms cannot be discounted. Indeed, our data show that PIP5KIβ is also retained by CR3 phagosomes. We were unable to determine whether PIP5KIα also behaves similarly because heterologous expression of this isoform often inhibited phagocytosis.

The appearance of $PI(3,4)P_2$ and $PI(3,4,5)P_3$ on phagosomes was accompanied by the recruitment of PBD-PAK1, a sensor of Rac and Cdc42 activation. Stimulation of Rac/Cdc42 is most likely caused by the phosphoinositides and mediates the formation of comet tails, a conclusion supported by the effects of wortmannin and LY294002 on actin recruitment. Accumulating evidence links the formation of 3′-polyphosphoinositides with the activation of Rho-family GTPases: not only are guanine nucleotide exchange factors such as P-Rex1 and Tiam1 stimulated by $PI(3,4,5)P_3$ (Fleming et al., 2000; Welch et al., 2002), but the phosphoinositide seems to directly bind and modulate the activity of Rac (Missy et al., 1998). The appearance of active Rac/Cdc42 on the phagosome is followed by the recruitment of actin, which initially surrounds the vacuole homogeneously. Shortly thereafter, however, the actin polarizes and gives rise to prominent comet tails that propel the phagosome, often toward the periphery of the cell. Neither the mechanism underlying the polarization of actin nor the consequences of phagosomal propulsion are known at present, although global inhibition of actin polymerization with latrunculin B did delay phagosome maturation. Displacement of the phagosome within the cell is likely to alter its ability to fuse with endomembranes and thus its maturation. The differential ability of FcγR- and CR3-induced phagosomes to generate actin comet tails may therefore be associated with differences in their rate or extent of maturation. Although we are not aware of studies systematically comparing the maturation of both types of phagosomes, it is noteworthy that pathogens like *Mycobacterium tuberculosis* manage to arrest phagosomal maturation at an early stage when entering macrophages via CR3, whereas they are delivered to phagolysosomes when using FcγR to enter (Armstrong and Hart, 1975; Schlesinger et al., 1990).

In summary, our findings revealed an unprecedented mechanism of PI(3)P-dependent actin polymerization associated with organellar motion and exposed sharp differences between phagosomes formed by CR3 and FcγR (Fig. 10). It is clear that the fate of phagosomes formed by engagement of different receptors varies and that additional differences will become apparent when other modes of phagocytosis are investigated in detail.

Materials and methods

Cell culture, plasmids, and transfection

Wild-type RAW264.7 macrophages obtained from American Type Culture Collection and RAW264.7 cells stably transfected with either mCherry-actin or GFP-actin (provided by D. Knecht, University of Connecticut, Storrs, CT) were grown in Dulbecco's modified Eagle's medium with 5% heat-inactivated FBS (Wisent). Cells plated on glass coverslips were transfected with Fugene HD (Roche) according to the manufacturer's instructions. In brief, each well of a 12-well plate was treated with 2 µg plasmid cDNA and 6 µl Fugene HD. Cells were used 24 h after transfection. The plasmids expressing the rapamycin heterodimerization system (PIP5K-FKBP–YFP, PIP5K(D253A)-FKBP–CFP, FKBP-YFP, and LDR) were provided by T. Meyer (Stanford University, Palo Alto, CA). The p85-YFP construct was provided by J. Swanson (University of Michigan, Ann Arbor, MI). The plasmid encoding the fusion of the PBD of PAK1 with YFP (PBD-PAK1–YFP) was a gift from the late G. Bokoch (Scripps Research Institute, La Jolla, CA). The $p40^{phox}$-PX domain vector was provided by M. Yaffe (Massachusetts Institute of Technology, Cambridge, MA). PIP5Kα-GFP, PIP5Kβ-GFP, and PIP5Kγ-GFP plasmids were supplied by P.D. Stahl (Washington University, St. Louis, MO). Rac1-DN–GFP and Cdc42-DN–GFP plasmids were furnished by M. Philips (New York University, New York, NY). GFP-PI4KIIA and GFP-PI4KIIB were gifts from H. Yin (University of Texas Southwestern, Dallas, TX). The vector pGEX-4T3-Gab2PHR32C was given by H. Gu (University of Colorado, Denver, CO). The mutated Gab2-PH domain was amplified (5′-TCACTCGAGCCCCGAATATGAGCGGC and 3′-ATCGGATCCTTAGAAGCCGCAGATCTGGCAG), digested with XhoI and BamHI (New England Biolabs, Inc.), and inserted into the plasmid pEGFP-C1 (Takara Bio Inc.). A positive clone, GFP–Gab2-PH(R32C), was confirmed with sequencing. The Inpp5B-GFP and GFP-APPL1 plasmids were gifts from P. De Camilli and D. Balkin (Yale University, New Haven, CT). The constructs encoding the

PH domain of PLCδ fused to GFP or RFP (PH-PLCδ–GFP and PH-PLCδ–RFP), two tandem PH domains of PLCδ fused to GFP (2PH-PLCδ–GFP), the PH domain of Akt fused to EGFP or RFP (PH-Akt–GFP and PH-Akt–RFP), GFP-Gab2, and the tandem FYVE domains (2FYVE-GFP and 5FYVE-GFP) were described previously (Stauffer et al., 1998; Marshall et al., 2001; Vieira et al., 2001; Gu et al., 2003; Mason et al., 2007).

Plasmid-cured *Y. pseudotuberculosis* (YP III p-; a gift from R. Isberg, Tufts University, Boston, MA) and *E. coli* (DH5α transformed with the pFPV25.1 plasmid to express EGFP under the control of the rpsM promoter) were grown overnight in Luria-Bertani medium at 37°C and were subcultured for 3 h before use. *S. cerevisiae* was grown overnight in rich YPD (yeast extract peptone dextrose) medium.

Live-cell imaging

Time-lapse images were acquired using a spinning-disk confocal microscopy system (Quorum) with a 63× oil immersion objective on a microscope (Axiovert 200M; Carl Zeiss, Inc.). Images were captured every 8 s for ∼15–20 min (unless otherwise specified) at 37°C with a back-thinned electron multiplier camera (C9100-13 ImagEM; Hamamatsu) and Volocity software (version 4.1.1; PerkinElmer). Images were analyzed with Volocity (version 5.3.2) and autocontrasted with Photoshop CS3 (Adobe). Cells were bathed in Hepes-buffered medium RPMI 1640 (Wisent) while imaging.

Phagocytosis assays

C3bi opsonization was performed by first incubating sheep RBCs (10% suspension; MP Biomedicals) with subagglutinating (1:10) concentrations of anti–sheep RBC IgM (Cedarlane Laboratories) in PBS with 0.5 mM $CaCl_2$ and 0.5 mM $MgCl_2$ for 1 h at room temperature under constant agitation. Excess IgM was then washed off, and the RBCs were incubated with human C5-deficient serum (1:6; Sigma-Aldrich) for 20 min at 37°C with frequent mixing. C3bi RBCs were then washed and used immediately. Where indicated, RBCs were labeled with $F(ab')_2$ anti–rabbit IgG (DyLight649; Jackson ImmunoResearch Laboratories, Inc.) that cross reacted with rabbit IgM. Other targets, including *Y. pseudotuberculosis*, GFP-expressing *E. coli*, zymosan, and *S. cerevisiae*, were incubated with complete human serum for 1 h at 37°C with frequent mixing and then washed in PBS containing calcium and magnesium. RAW264.7 cells were serum starved for 2 h and then incubated with 100 nM PMA (Bioshop) 20 min before the addition of C3bi-coated targets. Where indicated, the cells were treated with 100 nM wortmannin, 10 µM latrunculin B, 100 nM PI-103 (all three from EMD), 100 µM LY294002 (Enzo Life Science, Inc.), or 1 µM rapamycin (Sigma-Aldrich) shortly after phagocytosis was completed.

For FcγR-mediated phagocytosis, RBCs were opsonized with 1:50 anti–sheep RBC IgG (Cedarlane Laboratories) and incubated for 1 h at room temperature under constant agitation. Excess IgG was washed off, and RBCs were used immediately for phagocytosis.

Glass-bead loading

Acid-washed, 100-µm glass beads (Sigma-Aldrich) were alkali washed overnight in 4 M NaOH and then washed with distilled water until the pH of the water washes was stable near 7.0. RAW cells cultured on coverslips were rinsed three times with PBS and placed on an Attofluor chamber (Invitrogen). A small volume (80 µl) of PBS containing 32 µg anti-Vps34 antibody plus 80 µg rhodamine-labeled dextran (mol wt of 10,000; Invitrogen) was pipetted onto the culture, and beads were carefully and evenly sprinkled onto the coverslip, coating the entire surface. The beads were rolled two to four times from one side of the coverslip to the other with gentle rocking. The cells were next rinsed by dipping the coverslip in a PBS bath. Cultures were returned to the culture medium and allowed to recover at 37°C under 5% CO_2 for 20 min before use.

Online supplemental material

Fig. S1 shows that PBD-PAK1 accumulates transiently at sites of particle internalization and reassociates with recently formed phagosomes. Fig. S2 shows the specificity of the $PI(3,4,5)P_3$ probe during CR3-mediated uptake. Fig. S3 shows the effects of rapamycin-induced recruitment of PIP5KI-YFP or control YFP alone on $PI(3,4)P_2$/$PI(3,4,5)P_3$ and actin during FcRγ-mediated phagocytosis. Fig. S4 shows transient recruitment of APPL1 during CR3-mediated uptake. Video 1 shows formation of actin-rich pseudopods during CR3-mediated uptake. Video 2 shows actin surrounding the CR3-mediated phagosomes and coalescing to form a tail. Video 3 shows that actin tails are formed during phagocytosis of serum-opsonized yeast and *E. coli*. Video 4 shows distribution of PBD-PAK1, a probe for active Rac and Cdc42, during CR3-mediated phagocytosis. Video 5 shows that $PI(3,4)P_2$/$PI(3,4,5)P_3$ reaccumulates on sealed CR3-mediated phagosomes. Video 6 shows the tandem PH-PLCδ probe can detect $PI(4,5)P_2$ on CR3-mediated phagosomes. Video 7 shows that recruiting PIP5KI is sufficient to induce $PI(4,5)P_2$ accumulation on FcRγ-mediated phagosomes. Video 8 shows that recruiting PIP5KI to FcRγ-mediated phagosomes reproduces the actin tails seen during CR3-mediated phagocytosis. Video 9 shows that rapamycin-induced recruitment of a control (YFP) protein did not produce actin tails on FcRγ-mediated phagosomes. Video 10 shows that PI-103 selectively inhibits $PI(3,4,5)P_3$ formation without affecting PI(3)P synthesis. Online supplemental material is available at http://www.jcb.org/cgi/content/full/jcb.201004005/DC1.

We thank Dr. P. Leventis for performing some preliminary experiments leading to this work, Drs. G. Fairn and H. Sarantis for helping prepare the microbial targets, and Drs. P. De Camilli and D. Balkin for providing valuable advice and reagents.

This work was supported by the Canadian Institutes of Health Research grant MOP7075. G. Cosío was the recipient of a Consejo Nacional de Ciencia y Tecnología Fellowship. M. Bohdanowicz is the recipient of a Canadian Institutes of Health Research MD/PhD studentship and a McLaughlin Fellowship. S. Grinstein is the current holder of the Pitblado Chair in Cell Biology at the Hospital for Sick Children and is cross-appointed to the Department of Biochemistry (University of Toronto, Toronto, Canada).

Submitted: 1 April 2010
Accepted: 29 October 2010

References

Aderem, A., and D.M. Underhill. 1999. Mechanisms of phagocytosis in macrophages. *Annu. Rev. Immunol.* 17:593–623. doi:10.1146/annurev.immunol.17.1.593

Aoki, K., T. Nakamura, K. Fujikawa, and M. Matsuda. 2005. Local phosphatidylinositol 3,4,5-trisphosphate accumulation recruits Vav2 and Vav3 to activate Rac1/Cdc42 and initiate neurite outgrowth in nerve growth factor-stimulated PC12 cells. *Mol. Biol. Cell.* 16:2207–2217. doi:10.1091/mbc.E04-10-0904

Araki, N., M.T. Johnson, and J.A. Swanson. 1996. A role for phosphoinositide 3-kinase in the completion of macropinocytosis and phagocytosis by macrophages. *J. Cell Biol.* 135:1249–1260. doi:10.1083/jcb.135.5.1249

Armstrong, J.A., and P.D. Hart. 1975. Phagosome-lysosome interactions in cultured macrophages infected with virulent tubercle bacilli. Reversal of the usual nonfusion pattern and observations on bacterial survival. *J. Exp. Med.* 142:1–16. doi:10.1084/jem.142.1.1

Botelho, R.J., M. Teruel, R. Dierckman, R. Anderson, A. Wells, J.D. York, T. Meyer, and S. Grinstein. 2000. Localized biphasic changes in phosphatidylinositol-4,5-bisphosphate at sites of phagocytosis. *J. Cell Biol.* 151:1353–1368. doi:10.1083/jcb.151.7.1353

Caron, E., and A. Hall. 1998. Identification of two distinct mechanisms of phagocytosis controlled by different Rho GTPases. *Science.* 282:1717–1721. doi:10.1126/science.282.5394.1717

Choi, Y., Y. Lee, B.W. Jeon, C.J. Staiger, and Y. Lee. 2008. Phosphatidylinositol 3- and 4-phosphate modulate actin filament reorganization in guard cells of day flower. *Plant Cell Environ.* 31:366–377. doi:10.1111/j.1365-3040.2007.01769.x

Coppolino, M.G., R. Dierckman, J. Loijens, R.F. Collins, M. Pouladi, J. Jongstra-Bilen, A.D. Schreiber, W.S. Trimble, R. Anderson, and S. Grinstein. 2002. Inhibition of phosphatidylinositol-4-phosphate 5-kinase Ialpha impairs localized actin remodeling and suppresses phagocytosis. *J. Biol. Chem.* 277:43849–43857. doi:10.1074/jbc.M209046200

Erdmann, K.S., Y. Mao, H.J. McCrea, R. Zoncu, S. Lee, S. Paradise, J. Modregger, D. Biemesderfer, D. Toomre, and P. De Camilli. 2007. A role of the Lowe syndrome protein OCRL in early steps of the endocytic pathway. *Dev. Cell.* 13:377–390. doi:10.1016/j.devcel.2007.08.004

Fairn, G.D., K. Ogata, R.J. Botelho, P.D. Stahl, R.A. Anderson, P. De Camilli, T. Meyer, S. Wodak, and S. Grinstein. 2009. An electrostatic switch displaces phosphatidylinositol phosphate kinases from the membrane during phagocytosis. *J. Cell Biol.* 187:701–714. doi:10.1083/jcb.200909025

Fan, Q.W., Z.A. Knight, D.D. Goldenberg, W. Yu, K.E. Mostov, D. Stokoe, K.M. Shokat, and W.A. Weiss. 2006. A dual PI3 kinase/mTOR inhibitor reveals emergent efficacy in glioma. *Cancer Cell.* 9:341–349. doi:10.1016/j.ccr.2006.03.029

Fleming, I.N., A. Gray, and C.P. Downes. 2000. Regulation of the Rac1-specific exchange factor Tiam1 involves both phosphoinositide 3-kinase-dependent and -independent components. *Biochem. J.* 351:173–182. doi:10.1042/0264-6021:3510173

Franke, T.F., D.R. Kaplan, L.C. Cantley, and A. Toker. 1997. Direct regulation of the Akt proto-oncogene product by phosphatidylinositol-3,4-bisphosphate. *Science.* 275:665–668. doi:10.1126/science.275.5300.665

Gu, H., R.J. Botelho, M. Yu, S. Grinstein, and B.G. Neel. 2003. Critical role for scaffolding adapter Gab2 in FcγR-mediated phagocytosis. *J. Cell Biol.* 161:1151–1161. doi:10.1083/jcb.200212158

Hall, A.B., M.A. Gakidis, M. Glogauer, J.L. Wilsbacher, S. Gao, W. Swat, and J.S. Brugge. 2006. Requirements for Vav guanine nucleotide exchange factors and Rho GTPases in FcgammaR- and complement-mediated phagocytosis. *Immunity.* 24:305–316. doi:10.1016/j.immuni.2006.02.005

Hilpelä, P., M.K. Vartiainen, and P. Lappalainen. 2004. Regulation of the actin cytoskeleton by PI(4,5)P2 and PI(3,4,5)P3. *Curr. Top. Microbiol. Immunol.* 282:117–163.

Hinchliffe, K.A. 2001. Cellular signalling: stressing the importance of PIP3. *Curr. Biol.* 11:R371–R372. doi:10.1016/S0960-9822(01)00197-X

Inoue, T., W.D. Heo, J.S. Grimley, T.J. Wandless, and T. Meyer. 2005. An inducible translocation strategy to rapidly activate and inhibit small GTPase signaling pathways. *Nat. Methods.* 2:415–418. doi:10.1038/nmeth763

Kaplan, G. 1977. Differences in the mode of phagocytosis with Fc and C3 receptors in macrophages. *Scand. J. Immunol.* 6:797–807. doi:10.1111/j.1365-3083.1977.tb02153.x

Liebl, D., and G. Griffiths. 2009. Transient assembly of F-actin by phagosomes delays phagosome fusion with lysosomes in cargo-overloaded macrophages. *J. Cell Sci.* 122:2935–2945. doi:10.1242/jcs.048355

Lim, J., A. Wiedemann, G. Tzircotis, S.J. Monkley, D.R. Critchley, and E. Caron. 2007. An essential role for talin during alpha(M)beta(2)-mediated phagocytosis. *Mol. Biol. Cell.* 18:976–985. doi:10.1091/mbc.E06-09-0813

Ling, K., R.L. Doughman, A.J. Firestone, M.W. Bunce, and R.A. Anderson. 2002. Type I gamma phosphatidylinositol phosphate kinase targets and regulates focal adhesions. *Nature.* 420:89–93. doi:10.1038/nature01082

Loijens, J.C., I.V. Boronenkov, G.J. Parker, and R.A. Anderson. 1996. The phosphatidylinositol 4-phosphate 5-kinase family. *Adv. Enzyme Regul.* 36:115–140. doi:10.1016/0065-2571(95)00005-4

Marshall, J.G., J.W. Booth, V. Stambolic, T. Mak, T. Balla, A.D. Schreiber, T. Meyer, and S. Grinstein. 2001. Restricted accumulation of phosphatidylinositol 3-kinase products in a plasmalemmal subdomain during Fcγ receptor-mediated phagocytosis. *J. Cell Biol.* 153:1369–1380. doi:10.1083/jcb.153.7.1369

Mason, D., G.V. Mallo, M.R. Terebiznik, B. Payrastre, B.B. Finlay, J.H. Brumell, L. Rameh, and S. Grinstein. 2007. Alteration of epithelial structure and function associated with PtdIns(4,5)P2 degradation by a bacterial phosphatase. *J. Gen. Physiol.* 129:267–283. doi:10.1085/jgp.200609656

Missy, K., V. Van Poucke, P. Raynal, C. Viala, G. Mauco, M. Plantavid, H. Chap, and B. Payrastre. 1998. Lipid products of phosphoinositide 3-kinase interact with Rac1 GTPase and stimulate GDP dissociation. *J. Biol. Chem.* 273:30279–30286. doi:10.1074/jbc.273.46.30279

Pizarro-Cerdá, J., B. Payrastre, Y.J. Wang, E. Veiga, H.L. Yin, and P. Cossart. 2007. Type II phosphatidylinositol 4-kinases promote *Listeria* monocytogenes entry into target cells. *Cell. Microbiol.* 9:2381–2390. doi:10.1111/j.1462-5822.2007.00967.x

Rong, S.B., Y. Hu, I. Enyedy, G. Powis, E.J. Meuillet, X. Wu, R. Wang, S. Wang, and A.P. Kozikowski. 2001. Molecular modeling studies of the Akt PH domain and its interaction with phosphoinositides. *J. Med. Chem.* 44:898–908. doi:10.1021/jm000493i

Schlesinger, L.S., C.G. Bellinger-Kawahara, N.R. Payne, and M.A. Horwitz. 1990. Phagocytosis of *Mycobacterium tuberculosis* is mediated by human monocyte complement receptors and complement component C3. *J. Immunol.* 144:2771–2780.

Stauffer, T.P., S. Ahn, and T. Meyer. 1998. Receptor-induced transient reduction in plasma membrane PtdIns(4,5)P2 concentration monitored in living cells. *Curr. Biol.* 8:343–346. doi:10.1016/S0960-9822(98)70135-6

Underhill, D.M., and A. Ozinsky. 2002. Phagocytosis of microbes: complexity in action. *Annu. Rev. Immunol.* 20:825–852. doi:10.1146/annurev.immunol.20.103001.114744

Vieira, O.V., R.J. Botelho, L. Rameh, S.M. Brachmann, T. Matsuo, H.W. Davidson, A. Schreiber, J.M. Backer, L.C. Cantley, and S. Grinstein. 2001. Distinct roles of class I and class III phosphatidylinositol 3-kinases in phagosome formation and maturation. *J. Cell Biol.* 155:19–25. doi:10.1083/jcb.200107069

Welch, H.C., W.J. Coadwell, C.D. Ellson, G.J. Ferguson, S.R. Andrews, H. Erdjument-Bromage, P. Tempst, P.T. Hawkins, and L.R. Stephens. 2002. P-Rex1, a PtdIns(3,4,5)P3- and Gbetagamma-regulated guanine-nucleotide exchange factor for Rac. *Cell.* 108:809–821. doi:10.1016/S0092-8674(02)00663-3

Zhang, X., J.C. Loijens, I.V. Boronenkov, G.J. Parker, F.A. Norris, J. Chen, O. Thum, G.D. Prestwich, P.W. Majerus, and R.A. Anderson. 1997. Phosphatidylinositol-4-phosphate 5-kinase isozymes catalyze the synthesis of 3-phosphate-containing phosphatidylinositol signaling molecules. *J. Biol. Chem.* 272:17756–17761. doi:10.1074/jbc.272.28.17756

Zhou, Z., and X. Yu. 2008. Phagosome maturation during the removal of apoptotic cells: receptors lead the way. *Trends Cell Biol.* 18:474–485. doi:10.1016/j.tcb.2008.08.002

Zoncu, R., R.M. Perera, D.M. Balkin, M. Pirruccello, D. Toomre, and P. De Camilli. 2009. A phosphoinositide switch controls the maturation and signaling properties of APPL endosomes. *Cell.* 136:1110–1121. doi:10.1016/j.cell.2009.01.032